

## Description of ground-state band energies in well-deformed even-even nuclei with the confined $\beta$ -soft rotor model

K. Dusling and N. Pietralla

*Department of Physics & Astronomy, State University of New York, Stony Brook, New York 11794-3800, USA*

(Received 14 September 2004; revised manuscript received 24 January 2005; published 27 July 2005)

The analytical solution of the confined  $\beta$ -soft (CBS) rotor model is systematically compared to the energies of the ground-state rotational bands of strongly deformed heavy even-even nuclei. The model reproduces with one structural parameter the yrast band energies for all sufficiently well known rare-earth nuclei and actinides with a structural signature of  $R_{4/2} = E(4_1^+)/E(2_1^+) > 3.30$  up to the  $12^+$  state with an accuracy of the order of  $10^{-3}$ . This systematic study of the CBS model demonstrates the regularity of the ground-state bands without exception. Comparison to the Davydov Chaban model suggests that the agreement between data and collective models with soft potentials is insensitive to the details of the potential.

DOI: [10.1103/PhysRevC.72.011303](https://doi.org/10.1103/PhysRevC.72.011303)

PACS number(s): 21.10.Re, 21.60.Ev, 23.20.Lv, 27.70.+q

Many nuclei, particularly those close to midshell in the rare-earth and actinide regions, exhibit rotational character in the ground-state band [1,2]. However, deviations from the rigid rotor model's predictions for the level energies of the ground-state band increase for larger values of spin. The accuracy of the analytical rigid-rotor-model description is typically of the order of 1–10% for the members of the ground-state band (up to the  $10_1^+$  level). Numerous works [1–8] have analyzed these deviations from the rigid rotor model and they are usually attributed to collective effects such as centrifugal stretching or band-mixing and nonregularities resulting from the impact of noncollective microscopic degrees of freedom such as rotational alignment [3] or Coriolis antipairing [4–6]. There have also been many empirical models [7–9] that have added to our understanding of these irregularities. We are concerned here with a collective, purely geometrical approach in which microscopic degrees of freedom are not considered.

Much effort has recently been directed to understanding and predicting the characteristics of nuclei in regions of the nuclear chart where shape changes occur. Accurate spectroscopic data on transitional nuclei (e.g. [10,11]) and analytical solutions [12–14] of the Bohr Hamiltonian capable of describing nuclei near the critical points of the quadrupole-shape phase transitions have initiated a tremendous interest in the structure of transitional nuclei (e.g. [15–20] and references therein) and in the applicability of schematic square-well potentials in the deformation variable.

Iachello's analytical X(5) solution [13] of the Bohr Hamiltonian describes the situation close to the critical point of the transition from the spherical vibrator to the rigid rotor. The X(5) solution has been shown to satisfactorily predict the main features of the structure of nuclides with a structural signature  $R_{4/2} \equiv E(4_1^+)/E(2_1^+) \approx 2.9$  at or near the phase transitional point [11,21–24].

More recently the X(5) solution has been generalized to an analytical solution of the Bohr Hamiltonian for the full transition region between the critical point ( $R_{4/2} = 2.90$ ) and the rigid rotor limit ( $R_{4/2} = 10/3 \approx 3.333$ ) in terms of the confined  $\beta$ -soft (CBS) rotor model [20]. The latter parametrizes the width of an infinite-square-well potential

in the deformation variable  $\beta$  by allowing the boundaries of the square well to vary in the range  $0 \leq \beta_m \leq \beta \leq \beta_M$ . The ratio  $r_\beta = \beta_m/\beta_M \in [0, 1]$  serves as the structural parameter between X(5) ( $r_\beta = 0$ ) and the rigid rotor limit ( $r_\beta \rightarrow 1$ ). The CBS rotor model has already been shown to successfully describe the evolution of the  $\beta$  excitation from transitional nuclei at the critical point to moderately deformed rotors [20] as a function of the  $R_{4/2}$  value.  $\beta$  vibrations of strongly deformed nuclei have not yet been clearly identified [25] and are believed to exist at higher energies than the observed lowest lying  $K = 0$  state. In addition to the energy of the  $\beta$  excitation, the level energies within the yrast band itself depend sensitively on the softness of the nuclear quadrupole deformation, which can be modeled analytically with the CBS rotor model.

It is the purpose of this Rapid Communication to report on the description of the ground-state bands of strongly deformed nuclei systematically with the CBS model. The analytical energy expression of the CBS rotor model reproduces the yrast energy levels for all sufficiently deformed rare-earth nuclides and actinides with  $R_{4/2}$  ratios  $> 3.3$  up to the  $12_1^+$  level with an accuracy of about  $10^{-3}$  (i.e., *all* these ground bands follow the *same* energy formula with that accuracy). This excellent description demonstrates a regularity in the ground-state bands. Moreover, the ground-state band energies within the CBS model are compared to the model of Davydov Chaban (DC). Both models agree within 0.2% for the strongly deformed nuclei, showing that the description of ground-state-band energies is independent of the specific details of the potential in the deformation variable  $\beta$  as long as a sufficiently soft potential for  $\beta > 0$  has been chosen.

The CBS model [20] is an approximate analytical solution to the Bohr Hamiltonian in the quadrupole shape parameters  $\beta$  and  $\gamma$  with a separable potential of the form  $V(\beta, \gamma) = v(\beta) + u(\gamma)$ . For sufficiently axially symmetric prolate nuclei one might consider a steep harmonic oscillator in  $\gamma$  with  $\gamma \approx 0^\circ$ . By assuming a decoupling of the  $\beta$  and  $\gamma$  degrees of freedom the solution to the wave equation is of the form  $\Psi(\beta, \gamma, \theta_i) = \xi_L(\beta)\eta_K(\gamma)\mathcal{D}_{M,K}^L(\theta_i)$ , where  $\mathcal{D}$  denotes the Wigner functions with  $\theta_i$  being the Euler angles for the orientation of the intrinsic system, and  $\eta_K(\gamma)$  is the appropriate wave function in  $\gamma$  (e.g., a harmonic oscillator as considered in

Refs. [13,18]). The “radial” differential equation as a function of the shape parameter  $\beta$ ,

$$-\frac{\hbar^2}{2B} \left[ \frac{1}{\beta^4} \frac{\partial}{\partial \beta} \beta^4 \frac{\partial}{\partial \beta} - \frac{1}{3\beta^2} L(L+1) + u(\beta) \right] \xi_L(\beta) = E \xi_L(\beta), \quad (1)$$

contains the angular momentum dependence through the centrifugal term. The CBS rotor model assumes for prolate axially symmetric nuclides an infinite-square-well potential,  $u(\beta)$ , with boundaries at  $\beta_M > \beta_m \geq 0$ . For this potential the wave equation is analytically solvable [20]. The ratio  $r_\beta = \beta_m/\beta_M$  parametrizes the width of this potential (i.e., the stiffness of the nucleus in the  $\beta$  degree of freedom). For  $r_\beta = 0$  the X(5) limit is obtained with large fluctuations in  $\beta$ . The rigid rotor limit without fluctuations in  $\beta$  corresponds to  $r_\beta \rightarrow 1$ .

The quantization condition of the CBS rotor model is

$$Q_{\nu(L)}^{r_\beta}(z) = J_{\nu(L)}(z) Y_{\nu(L)}(r_\beta z) - J_{\nu(L)}(r_\beta z) Y_{\nu(L)}(z) = 0 \quad (2)$$

with  $J_\nu$  and  $Y_\nu$  being Bessel functions of first and second kind of irrational order  $\nu(L) = \sqrt{L(L+1)/3 + 9/4}$  (for states with  $K = 0$  on which we focus here). For a given structural parameter  $r_\beta$  and any spin value  $L$  the  $s$ th zero of Eq. (2) is denoted by  $z_{L,s}^{r_\beta}$ . The full solution of Eq. (1) with the aforementioned choice of CBS square-well potentials is then given as

$$\xi_{L,s}(\beta) = c_{L,s} \beta^{-3/2} \left[ J_\nu \left( z_{L,s}^{r_\beta} \frac{\beta}{\beta_M} \right) - \frac{J_\nu(r_\beta z_{L,s}^{r_\beta})}{Y_\nu(r_\beta z_{L,s}^{r_\beta})} Y_\nu \left( z_{L,s}^{r_\beta} \frac{\beta}{\beta_M} \right) \right] \quad (3)$$

with normalization

$$1/c_{L,s}^2 = \int_{\beta_m}^{\beta_M} \beta^4 [\xi_{L,s}(\beta)]^2 d\beta \quad (4)$$

and with the eigenvalues

$$E_{L,s} = \frac{\hbar^2}{2B\beta_M^2} (z_{L,s}^{r_\beta})^2. \quad (5)$$

The relative excitation energies thus depend on the structural parameter  $r_\beta$ , only. For the yrast band we have

$$R_{L/2} = \frac{E_x(L_1^+)}{E_x(2_1^+)} = \frac{(z_{L,1}^{r_\beta})^2 - (z_{0,1}^{r_\beta})^2}{(z_{2,1}^{r_\beta})^2 - (z_{0,1}^{r_\beta})^2}. \quad (6)$$

Figure 1 shows the wave functions for the  $0_1^+$  and the  $10_1^+$  states for a realistic structural parameter  $r_\beta = 0.45$ . The average deformation  $\langle \beta \rangle_L$  increases with angular momentum within the potential well owing to the presence of the centrifugal term in Eq. (1). As usual we refer to this phenomenon as *centrifugal stretching*. We stress that inclusion of the centrifugal term and the consistent quantum mechanical treatment of the chosen confined square-well potential are the only physics mechanisms in the model that cause the increase of the relative average deformation of the model’s wave functions with angular momentum.

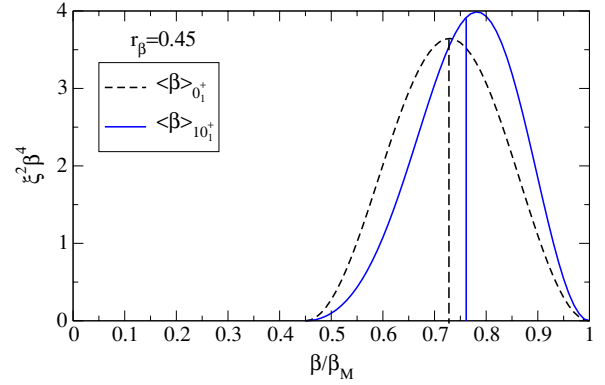


FIG. 1. (Color online) Wave function densities  $\xi_{L,s}^2 \beta^4$  from Eqs. (3) and (4) as a function of the deformation variable  $\beta$  and average deformation values  $\langle \xi | \beta | \xi \rangle$  for the  $L_s^\pi = 0_1^+$  ground state (dashed curve) and the  $10_1^+$  state (solid curve) for  $r_\beta = 0.45$ . The areas under the curves are normalized to one. The average deformation increases by about 5% from the  $0_1^+$  to the  $10_1^+$  state for this value of  $r_\beta$ .

We have carried out least-squares two-parameter fits of Eq. (5) to the data on yrast band energies [26] up to the  $12_1^+$  state for all sufficiently well known even-even nuclei with  $R_{4/2}$  values  $> 2.9$  from the cerium to the tungsten isotopic sequences. We have restricted the fit to this spin region to have a similar set of data for each nuclide considered and to safely stay below the back-bending region in all the nuclei. The essential structural parameter,  $r_\beta$ , defines the width of the square-well potential in  $\beta$  and, thus, the amount of centrifugal stretching in the ground-state band. The second parameter,  $\hbar^2/2B\beta_M^2$ , sets the energy scale. The fits were constrained to keep the fitted  $R_{4/2}$  value within 0.3% of the experimentally known value, that is, keep to deviations from the experimental value at 0.01 or less, because our analysis shows that  $R_{4/2}$  is significant at this level of accuracy. Figure 2 shows the experimental  $R_{12/2}$  (ratio of the energies of the first  $12^+$  to  $2^+$  levels of the ground-state band) as a function of  $r_\beta$  for rare-earth and actinide deformed nuclei ( $R_{4/2} > 2.9$ ). The solid curve shows the prediction of the CBS rotor model. Good agreement is seen between the ground-state band energy levels and the CBS rotor model for all transitional nuclei. Moreover, it is seen that the CBS rotor model can reproduce the ground-state band energies with sub-keV precision in nuclei with  $R_{4/2} > 3.30$  (dashed line in figure).

Table I shows the analytical results for the CBS model for the deformed Nd isotopes as examples. For reference we present also the prediction by the rigid rotor model using one parameter only [the energy scale fitted to  $E(2_1^+)$ ] instead of two (structural parameter  $r_\beta$  and scale). Similar results have been obtained for the Ce, Nd, Sm, Gd, Er, Yb, Hf, and W isotopic chains.

It is obvious from Table I that the CBS model describes the data much better than the rigid rotor. This is not surprising because the CBS has one parameter more than the rigid rotor, namely, the structural parameter  $r_\beta$  beside the energy scale. Thus it can account for deviations of the ground-state band energies from the rigid rotor predictions. Whereas the

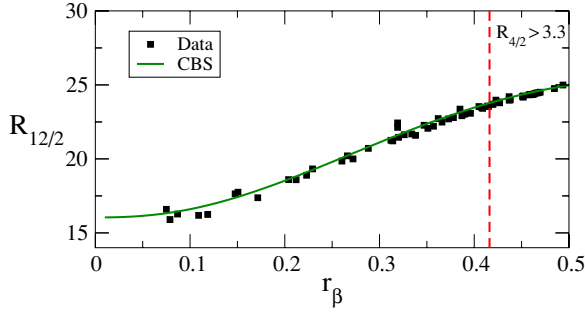


FIG. 2. (Color online) Correlation between  $R_{12/2}$  with  $r_{\beta}$  for deformed rare-earth and actinide nuclei with  $R_{4/2} > 2.9$  [26]. The solid curve shows the prediction of the CBS rotor model using the values of  $r_{\beta}$  determined in the procedure described earlier. Good agreement ( $\Delta E/E \leq 1-3\%$ ) is seen in the ground-state band for all transitional nuclei, whereas sub-keV precision is noticed above  $r_{\beta} > 0.42$ , corresponding to  $R_{4/2} > 3.30$  (dashed line).

CBS rotor yields a satisfactory description of the transitional nucleus  $^{150}\text{Nd}$  with deviations of a few parts in a thousand, the rigid rotor cannot reproduce the data (with typical deviations of 10% for  $J > 2$ ) because of the effects from the fluctuations in  $\beta$  caused by this nucleus being close to the spherical-to-deformed phase transitional point [21]. The accuracies of both the rigid rotor and CBS models increase when the  $R_{4/2}$  value increases. This is expected, of course, for the rigid rotor, because it yields always a fixed  $R_{4/2} = 10/3$ . Nonetheless, the deviations of the rigid rotor from the data on  $^{156}\text{Nd}$  amount to 1–5% for the  $4_1^+ - 10_1^+$  states.

In addition, the accuracy of the CBS rotor description increases with increasing  $R_{4/2}$ , which is interesting in itself given the schematic character of the CBS square-well potential. This level of accuracy obtained is remarkable, as is seen in the level energies in  $^{156}\text{Nd}$  which are described with sub-keV precision

TABLE I. Yrast band energies of Nd nuclei with  $R_{4/2} > 2.9$  compared to the CBS and rigid rotor models.

$J$	CBS	Expt.	Rigid rotor	CBS	Expt.	Rigid rotor
	$^{150}\text{Nd}$ $R_{4/2} = 2.929$			$^{152}\text{Nd}$ $R_{4/2} = 3.263$		
$2_1^+$	130.3	130.2	130.2	72.7	72.5	72.5
$4_1^+$	382.8	381.5	434.0	237.9	236.6	241.7
$6_1^+$	718.6	720.4	911.5	486.3	484.0	507.6
$8_1^+$	1124.6	1129.7	1562.5	807.0	805.4	870.1
$10_1^+$	1595.8	1599.0	2387.2	1190.3	1195.3	1329.4
$12_1^+$	2129.5	2119.0	3385.5	1629.6	1647.6	1885.3
	$^{154}\text{Nd}$ $R_{4/2} = 3.294$			$^{156}\text{Nd}$ $R_{4/2} = 3.315$		
$2_1^+$	70.8	70.8	70.8	66.9	66.9	66.9
$4_1^+$	233.4	233.2	236.0	221.6	221.8	223.0
$6_1^+$	482.5	481.9	495.6	460.3	460.4	468.3
$8_1^+$	810.7	810.1	849.6	778.3	777.9	802.8
$10_1^+$	1210.2	1210.8	1298.0	1169.6	1168.9	1226.5
$12_1^+$	1674.0	1677.3	1840.8	1628.5	1628.4	1739.4

TABLE II. Yrast band energies of six rare-earth nuclei with  $R_{4/2} > 3.3$  compared to the CBS model prediction.  $R_{4/2}$  values of a given nucleus are given in parenthesis.

$J$	CBS	Expt.	CBS	Expt.	CBS	Expt.
	$^{158}\text{Sm}$ (3.301)		$^{160}\text{Gd}$ (3.302)		$^{164}\text{Dy}$ (3.301)	
$2_1^+$	72.7	72.8	75.2	75.3	73.4	73.4
$4_1^+$	240.7	240.3	248.6	248.5	242.3	242.2
$6_1^+$	499.7	498.4	515.2	514.8	501.4	501.3
$8_1^+$	843.9	844.5	868.3	867.9	843.5	843.7
$10_1^+$	1266.6	1266.7	1300.4	1300.7	1260.7	1261.3
$12_1^+$	1761.4	1765.8	1804.2	1806.3	1745.9	1745.9
	$^{170}\text{Er}$ (3.310)		$^{174}\text{Yb}$ (3.310)		$^{180}\text{Hf}$ (3.307)	
$2_1^+$	78.6	78.6	76.5	76.5	93.3	93.3
$4_1^+$	260.2	260.1	253.2	253.1	308.8	308.6
$6_1^+$	541.0	540.7	526.0	526.0	641.6	640.9
$8_1^+$	915.2	915.0	889.4	889.9	1084.6	1083.9
$10_1^+$	1376.2	1376.6	1336.6	1336.	1629.8	1630.4
$12_1^+$	1917.3	1918.7	1861.0	1861.	2269.0	2272.4

up to the  $12_1^+$  state at 1.6 MeV. Deviations are  $< 10^{-3}$ , one to two orders of magnitude smaller than for the rigid rotor.

One might think that this precise description of  $^{156}\text{Nd}$  could be accidental. However, Eq. (6) describes the ground bands of *all* well-deformed nuclei with a similar precision.  $^{156}\text{Nd}$  has an  $R_{4/2}$  ratio of 3.315. We analyzed the ground-state bands up to the  $12_1^+$  state for all rare-earth nuclei with  $R_{4/2} > 3.30$  for which sufficient data were available and on which the remaining part of this paper is focused. From a data search in the National Nuclear Data Center [26] one finds 13 nuclides that satisfy that condition:  $^{156}\text{Nd}$ ,  $^{158}\text{Sm}$ ,  $^{160}\text{Gd}$ ,  $^{164,166}\text{Dy}$ ,  $^{168,170,172}\text{Er}$ ,  $^{172,174,176,178}\text{Yb}$ , and  $^{180}\text{Hf}$ . These nuclei belong to seven different isotopic chains and to seven different isotonic sequences ( $N = 96, 98, 100, 102, 104, 106$ , and  $108$ ). Table II shows the data for 6 of these 13 nuclei.

The accuracy of the CBS description is similar to the case of  $^{156}\text{Nd}$  for all 13 rare-earth nuclei with  $R_{4/2} > 3.30$  with no exception. Deviations are typically  $< 10^{-3}$ . The accurate description of ground-state band energies is not limited to the strongly deformed rare-earth nuclei. Equation (6) accounts for the data with an accuracy of better than one part in a thousand for the  $2_1^+ - 12_1^+$  energies in strongly deformed actinides.

To further quantify the regularity of the studied ground-state bands we consider the level energies as sums of collective (regular) and noncollective (irregular) parts,  $E(J) = E_{\text{coll}}(J) + \delta E_{\text{ncoll}}(J)$ . The average *irregularity* of a ground-state band may then be defined as

$$I = \frac{1}{n(J)} \sum \frac{|\delta E_{\text{ncoll}}(J)|}{E(J)}. \quad (7)$$

Making the ansatz  $E_{\text{coll}}(J) \approx E_{\text{CBS}}(J)$  we consider

$$I_{\text{CBS}} = \frac{1}{n(J) - 1} \sum \frac{|E(J) - E_{\text{CBS}}|}{E(J)} \quad (8)$$

TABLE III. Experimental and CBS  $R_{4/2}$  values for all well-known strongly deformed rare-earth and actinide nuclei. Values of  $I_{\text{CBS}}$  are also given.

Nuclide	$R_{4/2}^{\text{expt}}$	$R_{4/2}^{\text{CBS}}$	$r_\beta$	$I_{\text{CBS}} (10^{-3})$
$^{156}\text{Nd}$	3.315	3.310	0.460	0.56
$^{158}\text{Sm}$	3.301	3.308	0.452	1.63
$^{160}\text{Gd}$	3.302	3.305	0.438	0.73
$^{164}\text{Dy}$	3.301	3.301	0.427	0.26
$^{166}\text{Dy}$	3.307	3.311	0.463	0.55
$^{168}\text{Er}$	3.318	3.311	0.462	0.96
$^{170}\text{Er}$	3.310	3.311	0.464	0.45
$^{172}\text{Er}$	3.305	3.312	0.468	1.00
$^{172}\text{Yb}$	3.305	3.308	0.451	0.86
$^{174}\text{Yb}$	3.310	3.310	0.460	0.24
$^{176}\text{Yb}$	3.308	3.308	0.452	0.98
$^{178}\text{Yb}$	3.310	3.316	0.485	2.18
$^{180}\text{Hf}$	3.307	3.310	0.459	0.95
$^{236}\text{U}$	3.304	3.305	0.438	0.24
$^{238}\text{U}$	3.303	3.304	0.437	0.40
$^{238}\text{Pu}$	3.311	3.313	0.470	0.70
$^{240}\text{Pu}$	3.309	3.310	0.458	0.46
$^{242}\text{Pu}$	3.307	3.310	0.460	0.38

as an upper limit for the average irregularity of the studied part of the band. This takes into account that one structural parameter ( $r_\beta$ ) has been fitted to the relative excitation energies. Table III shows the experimental and CBS  $R_{4/2}$  values and irregularities for all 18 nuclei. The high accuracy of the CBS rotor model can be seen from this table;  $I_{\text{CBS}}$  is on the order of  $10^{-3}$  for all 18 strongly deformed nuclei.

An important test for the modeling of centrifugal stretching is its predictive power for  $E2$  transition rates within the rotational bands as a function of spin. Centrifugal stretching of the nucleus causes the average deformation  $\langle\beta\rangle_L$  of the wave function to tend toward larger values with increasing spin causing an increase in the transitional quadrupole moment ( $Q_t \propto \langle L_f | \beta | L_i \rangle$ ) along the ground-state band. The CBS model predicts an increase in  $Q_t$  by 3.9% from  $J = 2$  to  $J = 10$  for  $r_\beta = 0.45$  (note that the increase of  $Q_t$  differs slightly from the increase of the average deformation because the latter corresponds to a diagonal matrix element of  $\hat{\beta}$  and the former involves two different wave functions for the initial and final state). Figure 3 shows typical experimental  $Q_t$  values, here as an example for  $^{152}\text{Sm}$  and  $^{172}\text{Yb}$ , with both the predictions made by the rigid rotor and CBS rotor model. Centrifugal stretching is clearly observed for the transitional nucleus  $^{152}\text{Sm}$ . The data are in full agreement with the model prediction using the  $E2$  operator up to second order in  $\beta$  [20]. Unfortunately, the change in  $Q_t$  values of more rigidly deformed nuclei is predicted to be considerably smaller such that the present data on lifetimes in strongly deformed nuclei are not accurate enough for testing this model prediction with sufficient accuracy. The data certainly do not contradict geometrical models.

Centrifugal stretching has previously been modeled geometrically in many ways (e.g., by Davydov and Chaban). It is interesting to consider the model of DC [29] for the description

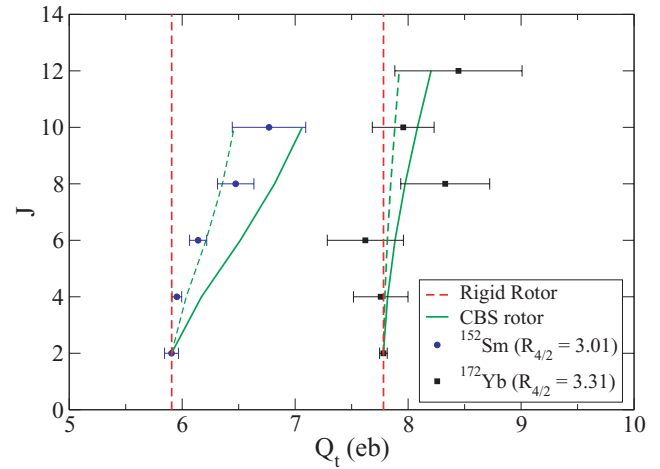


FIG. 3. (Color online)  $Q_t$  values as a function of spin determined by experimental  $B(E2)$  values of  $^{152}\text{Sm}$  [27,28] and  $^{172}\text{Yb}$  [26] that are representative for the quality of  $E2$  data for the ground-state bands of rare-earth nuclei. The dashed lines show the rigid rotor prediction and the solid curves show predictions by the CBS rotor model where the  $E2$  operator is considered here in lowest order in  $\beta$  [ $T(E2) \propto \beta$ ] for simplicity (see Ref. [20] for the definition of the  $E2$  operator up to second order). An increase of  $Q_t$  is clearly observed for the less rigidly deformed nucleus where the effects are larger and easier to measure.  $Q_t$  values including a second-order correction ( $\chi = -0.535$  [20]) in the  $E2$  operator are shown by the dashed curves.

of these ground-state band energies, too. We use the limit of  $\gamma = 0$  and fit the “nonadiabaticity” parameter  $\mu$  and the energy scale to the data in a fashion as was done before. Similar analysis has been done on other axially symmetric nuclei in [30]. Table IV shows a comparison of the relative ground-state band energies from the CBS and the DC models as calculated by a fit to  $R_{4/2}$ . For  $R_{4/2} > 3.30$  the predictions of the two models coincide within 0.2% up to  $J = 12^+$ .

In both the CBS and DC models it is the centrifugal stretching that causes the change of shape in the nucleus at higher spins, thus leading to an increase in the moment of inertia with spin. Since both of these models describe the nuclei in the rare-earth region so well, it is concluded that centrifugal stretching is the dominant mechanism causing the deviations from the rigid rotor. This is achieved without any fine-tuning of the potentials. The new aspect provided by our study is the observation that the precision of the description of data is systematical and does not depend much on the details of the potential nor on the treatment of the  $\gamma$  degree of freedom.

We have demonstrated that ground-state bands of strongly deformed even-even nuclei in the rare-earth and actinide regions with  $R_{4/2}$  values  $> 3.30$  follow the analytical energy formula of the CBS rotor model or the DC model for  $\gamma = 0$  systematically within a precision of about 1/1000 (at least up to the  $10_1^+$  state). We stress that *all* these nuclei follow the *same* energy formula at this level of accuracy. This demonstrates that the ground-state bands of strongly deformed nuclei exhibit a regularity at least down to the order of  $10^{-3}$ . Collective nuclear structure models such as DC and the CBS rotor model

TABLE IV. Relative ground-state band energies as predicted by both the CBS and DC models. Agreement between the models is seen to 0.2%.

$J$	$R_{4/2} = 3.20$		$R_{4/2} = 3.30$		$R_{4/2} = 3.32$	
	CBS	DC	CBS	DC	CBS	DC
	$r_\beta = 0.274$	$\mu = 0.268$	$r_\beta = 0.425$	$\mu = 0.188$	$r_\beta = 0.510$	$\mu = 0.151$
$2_1^+$	1	1	1	1	1	1
$4_1^+$	3.200	3.200	3.300	3.300	3.320	3.320
$6_1^+$	6.370	6.382	6.828	6.830	6.929	6.930
$8_1^+$	10.316	10.341	11.483	11.495	11.782	11.785
$10_1^+$	14.930	14.920	17.157	17.190	17.819	17.830
$12_1^+$	20.166	20.005	23.753	23.816	24.976	25.004

describe these data equally well, despite the fact that the treatment of the centrifugal term and the form of the potentials differ. They have in common a description of the centrifugal stretching of the rotating nucleus as a function of spin. This strongly supports the conclusion that centrifugal stretching is the dominant mechanism for the deviation of the ground-state band energies from the rigid rotor prediction for the strongly deformed nuclei with  $R_{4/2} > 3.30$ . We stress that the accurate predictions of relative excitation energies for the levels in the

ground-state band of strongly deformed nuclei are typically better than one part in a thousand, belonging to the most precise predictions in nuclear physics. New types of highly accurate  $B(E2)$  measurements are very desirable for testing these conclusions that are based on energies.

We thank F.S. Stephens for discussions. This work is supported by NSF Grant No. PHY 0245018 and by DOE Grant No. DE-FG02-04ER41334.

- 
- [1] A. Bohr, *Mat. Fys. Medd. K. Dan. Vidensk Selsk.* **26**, (14) (1952).
- [2] A. Bohr and B. Mottelson, *Nuclear Structure II* (Benjamin, Reading, 1975).
- [3] F. S. Stephens, *Rev. Mod. Phys.* **47**, 43 (1975).
- [4] M. W. Guidry *et al.*, *Phys. Rev. C* **20**, 1814 (1979).
- [5] B. R. Mottelson and J. G. Valatin, *Phys. Rev. Lett.* **5**, 511 (1960).
- [6] M. J. A. de Voigt, J. Dudek, and Z. Szymanski, *Rev. Mod. Phys.* **55**, 949 (1983).
- [7] M. A. J. Mariscotti, G. Scharff-Goldhaber, and B. Buck, *Phys. Rev.* **178**, 1864 (1964).
- [8] S. M. Harris, *Phys. Rev.* **138**, B509 (1965).
- [9] P. von Brentano, N. V. Zamfir, R. F. Casten, W. G. Rellergert, and E. A. McCutchan, *Phys. Rev. C* **69**, 044314 (2004).
- [10] R. F. Casten, M. Wilhelm, E. Radermacher, N. V. Zamfir, and P. von Brentano, *Phys. Rev. C* **57**, R1553 (1998).
- [11] R. F. Casten and N. V. Zamfir, *Phys. Rev. Lett.* **87**, 052503 (2001).
- [12] F. Iachello, *Phys. Rev. Lett.* **85**, 3580 (2000).
- [13] F. Iachello, *Phys. Rev. Lett.* **87**, 052502 (2001).
- [14] F. Iachello, *Phys. Rev. Lett.* **91**, 132502 (2003).
- [15] J. Jolie, R. F. Casten, P. von Brentano, and V. Werner, *Phys. Rev. Lett.* **87**, 162501 (2001).
- [16] N. V. Zamfir, P. von Brentano, R. F. Casten, and J. Jolie, *Phys. Rev. C* **66**, 021304(R) (2002).
- [17] A. Leviatan and J. N. Ginocchio, *Phys. Rev. Lett.* **90**, 212501 (2003).
- [18] R. Bijker, R. F. Casten, N. V. Zamfir, and E. A. McCutchan, *Phys. Rev. C* **68**, 064304 (2003).
- [19] F. Iachello and N. V. Zamfir, *Phys. Rev. Lett.* **92**, 212501 (2004).
- [20] N. Pietralla and O. M. Gorbachenko, *Phys. Rev. C* **70**, 011304(R) (2004).
- [21] R. Krücken *et al.*, *Phys. Rev. Lett.* **88**, 232501 (2002).
- [22] M. A. Caprio *et al.*, *Phys. Rev. C* **66**, 054310 (2002).
- [23] D. Tonev, A. Dewald, T. Klug, P. Petkov, J. Jolie, A. Fitzler, O. Möller, S. Heinze, P. von Brentano, and R. F. Casten, *Phys. Rev. C* **69**, 034334 (2004).
- [24] R. M. Clark *et al.*, *Phys. Rev. C* **68**, 037301 (2003).
- [25] P. E. Garrett, *J. Phys. G* **27**, R1 (2001).
- [26] National Nuclear Data Center, Brookhaven National Laboratory, <http://www.nndc.bnl.gov/>, 2004.
- [27] N. V. Zamfir *et al.*, *Phys. Rev. C* **60**, 054312 (1999), and references therein.
- [28] C. W. Reich and R. G. Helmer, *Nucl. Data Sheets* **85**, 171 (1998).
- [29] A. S. Davydov and A. A. Chaban, *Nucl. Phys.* **20**, 499 (1960).
- [30] F. S. Stephens, N. Lark, and R. M. Diamond, *Phys. Rev. Lett.* **12**, 225 (1964).